Performance Analysis of Full-Duplex Relaying with Media-Based Modulation

Yalagala Naresh and A. Chockalingam

Department of ECE, Indian Institute of Science, Bangalore 560012

Abstract—In this paper, we analyze the performance of a two-hop three-node full-duplex (FD) relay network, where the source and relay nodes transmit using media-based modulation (MBM). MBM is a promising new modulation scheme that conveys information bits by digitally controlling the parasitic elements (called as radio frequency mirrors) placed near the transmit antenna. The relay uses decode-and-forward relaying protocol. We refer to this system as FD relaying with MBM (FDR-MBM) system. First, we derive an upper bound on the end-to-end average bit error probability of FDR-MBM with maximum-likelihood (ML) detection at the relay and destination nodes. This bound is shown to be increasingly tight with increasing signal-to-noise ratio. Our numerical results show that, for the same spectral efficiency, FDR-MBM can perform better than FD relaying with conventional modulation schemes such as QAM/PSK. Next, we derive the diversity order achieved by the FDR-MBM system. Also, the analytically predicted diversity order is validated through simulations.

Keywords – Full-duplex, relay networks, media-based modulation, performance analysis.

I. INTRODUCTION

Full-duplex (FD) communication has gained a lot of research interest due to its capability of achieving higher spectral efficiency compared to half-duplex (HD) communication [1],[2]. In FD, a communication node transmits and receives simultaneously over the same frequency band as opposed to that in HD, where a node can transmit and receive either at different times over the same frequency band or at the same time over different frequency bands. However, the performance of FD systems is limited by the self-interference (SI) caused by the signal leakage from a node's transmitter to its own receiver. Several cancellation techniques have been proposed in the literature to mitigate the SI. These techniques are classified mainly into passive and active cancellation techniques [3]. However, in practice, these cancellation techniques cannot mitigate the SI completely. Several studies on FD have explicitly considered the effect of imperfect SI cancellation, where residual SI is modeled as either Rician or Rayleigh random variable whose variance depends on the average transmitted power [4],[5]. The performance of the FD systems with multiple transmit and receive antennas at communication nodes have been reported in [5].

Relaying is an attractive technique that can improve the network coverage, quality-of-service (QoS), and throughput in wireless networks. Amplify-and-forward (AF) and decode-and-forward (DF) protocols are commonly studied relaying

protocols [6]. The FD operation of nodes in relay networks has been shown to provide higher network spectral efficiency compared to HD relaying [7]-[11]. Most studies on FD relay systems reported in the literature employ either conventional modulation schemes such as QAM/PSK [8] or spatial modulation [11]. In this paper, we consider *FD relaying with a new modulation scheme, known as the media-based modulation (MBM)*, which is a promising modulation scheme in rich scattering environments [12],[13].

The concept of MBM can be briefly explained as follows. In MBM, digitally controllable parasitic elements (e.g., varactors, switched capacitors) are placed near the transmit antenna as radio frequency (RF) mirrors. Each RF mirror can be either ON or OFF. A mirror allows the incident RF signal to pass through transparently when it is ON and reflects back the incident RF signal when it is OFF, i.e., RF mirror act as a controlled signal scatterer in the propagation environment close to the transmit antenna. The ON/OFF status of the mirrors is called as 'mirror activation pattern (MAP)'. If there are m_{rf} mirrors, then $2^{m_{rf}}$ MAPs are possible. Since the ON/OFF mirrors change from one MAP to the other, the propagation environment near the transmit antenna becomes different for different MAPs. This results in different fade realizations for different MAPs. The collection of $2^{m_{rf}}$ such fades corresponding to different MAPs form the MBM channel alphabet. This MBM alphabet is used to convey m_{rf} information bits. The transmit antenna transmits a symbol from a conventional modulation alphabet (e.g., QAM) to convey additional information bits.

MBM has been shown to perform significantly better than conventional modulation schemes [12],[13]. The performance of MBM in a point-to-point FD communication setting has been studied in [14]. In this paper, *for the first time in the literature, we analyze the performance of a two-hop full-duplex relay (FDR) network with MBM* (referred to as FDR-MBM). We consider generalized spatial modulation MBM (GSM-MBM) [13] for transmission at the source and relay nodes, and DF protocol for relaying. We refer to two-hop FD relaying with conventional modulation as FDR-CM system. Our contributions in this paper can be summarized as follows.

- First, we derive an upper bound on the end-to-end average bit error probability (BEP) of FDR-MBM with maximum-likelihood (ML) detection at the relay and destination nodes. This bound is shown to be tight for moderate to high signal-to-noise ratios (SNRs). Our simulation results show that, for the same spectral efficiency, FDR-MBM can perform better than FDR-CM.
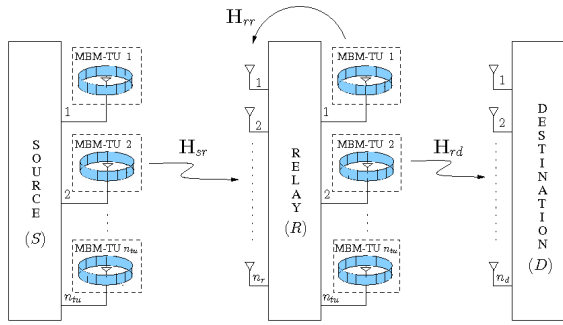
Fig. 1. Full-duplex relaying with MBM.

- Next, we derive the diversity order achieved by the FDR-MBM system which is given by $\min\{n_r \min\{\lambda, 1\}, n_d\}$, where λ is a constant that captures the quality of SI cancellation, n_r and n_d are the number of receive antennas at the relay and the destination, respectively. This diversity order is also validated through simulations.

II. SYSTEM MODEL

Consider a two-hop relay network consisting of a HD source node S, a FD relay node R, and a HD destination node D as shown in Fig. 1. The relay and destination nodes are equipped with n_r and n_d receive antennas, respectively. The source and relay nodes are equipped with n_{tu} MBM-TUs, and n_{rf} RF chains, $1 \leq n_{rf} \leq n_{tu}$. We assume that the source and destination can communicate only through the relay, i.e., there is no direct link between the source and destination. The relay uses DF protocol. The transmitter at the source and relay use GSM-MBM.

A. GSM-MBM transmitter at source and relay

The GSM-MBM transmitter is shown in Fig. 2. Information bits are conveyed using MBM-TU indexing, RF mirror indexing, and QAM/PSK symbols, as follows. In each channel use, i) n_{rf} out of n_{tu} MBM-TUs are selected using $\lfloor \log_2 \binom{n_{tu}}{n_{rf}} \rfloor$ bits, ii) n_{rf} M-ary QAM/PSK symbols (formed using $n_{rf} \log_2 M$ bits) are transmitted on the selected n_{rf} MBM-TUs, and iii) the m_{rf} mirrors in each of the selected MBM-TU are controlled (made ON/OFF) by m_{rf} bits (so that all the $n_{rf}m_{rf}$ mirrors in the selected n_{rf} MBM-TUs are controlled by $n_{rf}m_{rf}$ bits). Therefore, the achieved rate, in bits per channel use (bpcu), is given by

$$\eta = \underbrace{\left\lfloor \log_2 \binom{n_{tu}}{n_{rf}} \right\rfloor}_{\text{MBM-TU index bits}} + \underbrace{n_{rf}m_{rf}}_{\text{mirror index bits}} + \underbrace{n_{rf} \log_2 M}_{\text{QAM/PSK symbol bits}} \quad \text{bpcu.} \quad (1)$$

It is noted that GSM-MBM specializes to other MBM schemes, such as SIMO-MBM when $n_{tu} = n_{rf} = 1$, spatial modulation MBM (SM-MBM) when $n_{tu} > 1$ and $n_{rf} = 1$, and MIMO-MBM when $n_{tu} > 1$ and $n_{rf} = n_{tu}$.

In a given channel use, n_{rf} out of the n_{tu} MBM-TUs are made ON (and on MBM-TU that is made ON, a symbol from M-ary QAM/PSK alphabet $\mathbb{A}$ is sent) and the remaining

MBM-TU stands for MBM transmit unit comprising of a transmit antenna and m_{rf} RF mirrors placed near it.

$n_{tu} - n_{rf}$ MBM-TUs are made OFF (which is equivalent to sending 0). A realization of the ON/OFF status of the n_{tu} MBM-TUs (which is a $n_{tu} \times 1$ vector consisting of 1's and 0's, where 1 or 0 in a coordinate represent the ON or OFF status of the MBM-TU corresponding to that coordinate, respectively) is called as a 'MBM-TU activation pattern'. A total of $\binom{n_{tu}}{n_{rf}}$ MBM-TU activation patterns are possible. Out of them, only $2^{\lfloor \log_2 \binom{n_{tu}}{n_{rf}} \rfloor}$ are needed for signaling. Let $\mathbb{S}_t$ denote the set of these $2^{\lfloor \log_2 \binom{n_{tu}}{n_{rf}} \rfloor}$ MBM-TU activation patterns chosen from the set of all possible MBM-TU activation patterns. For example, for $n_{tu} = 4$, $n_{rf} = 2$, a possible $\mathbb{S}_t$ is given by

$$\mathbb{S}_t = \{[1\ 1\ 0\ 0]^T, [0\ 1\ 1\ 0]^T, [0\ 0\ 1\ 1]^T, [1\ 0\ 0\ 1]^T\}.$$

A mapping is done between the combinations of $\lfloor \log_2 \binom{n_{tu}}{n_{rf}} \rfloor$ bits to the MBM-TU activation patterns in $\mathbb{S}_t$. Let s_j denote the symbol transmitted on the jth MBM-TU. Then $s_j \in \mathbb{A} \cup \{0\}$ such that $\|\mathbf{s}\|_0 = n_{rf}$ and $\mathcal{I}(\mathbf{s}) \in \mathbb{S}_t$, where $\mathbf{s} = [s_1\ s_2\ \ldots\ s_{n_{tu}}]^T$, $\|\mathbf{s}\|_0$ denotes the number of non-zero elements in $\mathbf{s}$, and $\mathcal{I}(\mathbf{s})$ is a function that gives the MBM-TU activation pattern for $\mathbf{s}$. For example, when $\mathbb{A}$ is BPSK, $n_{tu} = 4$, $n_{rf} = 2$, and $\mathbf{s} = [+1\ 0\ 0\ -1]^T$, then $\mathcal{I}(\mathbf{s})$ in this case is given by $\mathcal{I}(\mathbf{s} = [+1\ 0\ 0\ -1]^T) = [1\ 0\ 0\ 1]^T$. Let $\mathbb{S}_{\text{gsm}}$ denote the set of such $\mathbf{s}$ vectors, i.e., $\mathbb{S}_{\text{gsm}} = \{\mathbf{s} : s_j \in \mathbb{A} \cup \{0\}, \|\mathbf{s}\|_0 = n_{rf}, \mathcal{I}(\mathbf{s}) \in \mathbb{S}_t\}$.

In each of the n_{tu} MBM-TUs, an RF mirror can be made either ON or OFF. An m_{rf}-length vector of the ON/OFF status of the m_{rf} mirrors is called as a 'mirror activation pattern (MAP)'. Since each mirror can be either ON or OFF, a total of $N_m = 2^{m_{rf}}$ MAPs are possible. A mapping is done between the combinations of m_{rf} information bits and the MAPs. This mapping is made known a priori at all the nodes for encoding and decoding purposes, respectively. Let l_j denote the index of the MAP chosen on the jth MBM-TU. The MAP index l_j is selected as follows: i) when $s_j \neq 0$ (i.e., MBM-TU is ON), l_j takes an integer value in $[1, N_m]$, based on m_{rf} information bits; ii) otherwise $l_j = 1$, which does not convey any information.

B. Transmission protocol

The relay operates in FD mode and uses DF protocol. The information is conveyed from the source to the destination in two phases. In the first phase, the source transmits its information to the relay. The relay detects the data in the presence of SI (which is transmitted to the destination by the relay) that results from the FD operation of the relay. In the next phase, the relay forwards the detected data to the destination and simultaneously receives a new information from the source. We assume that both source and relay use the same average power denoted by E. Note that relay operates in HD mode (only receives the data from the source) at the first instance of the transmission, because it does not have any data to forward to the destination.

C. Channel model

The source-to-relay (S to R), relay-to-destination (R to D), and relay-to-relay SI (R to R-SI) channels are assumed to experience independent fading.
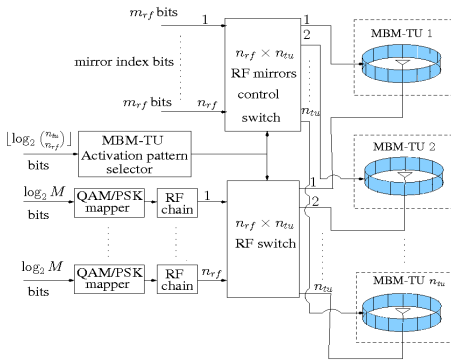
Fig. 2. GSM-MBM transmitter.

S to R channel: Let $\mathbf{h}_k^{j,sr} = [h_{1,k}^{j,sr} \ h_{2,k}^{j,sr} \ \cdots \ h_{n_r,k}^{j,sr}]^T$ denote the $n_r \times 1$-sized channel gain vector at the receiver of the relay node corresponding to the kth MAP of the jth MBM-TU of the source node, where $h_{i,k}^{j,sr}$ is the fade coefficient corresponding to the kth MAP of jth MBM-TU of the source to the ith receive antenna of the relay, $i = 1, 2, \cdots, n_r$, $j = 1, 2, \cdots, n_{tu}$, and $k = 1, 2, \cdots, N_m$. The $h_{i,k}^{j,sr}$s are assumed to be independent and identically distributed (i.i.d.) and distributed as $\mathcal{CN}(0,1)$. Let $\mathbb{H}_{sr}^j = \{\mathbf{h}_1^{j,sr}, \mathbf{h}_2^{j,sr}, \cdots, \mathbf{h}_{N_m}^{j,sr}\}$ denote the MBM channel alphabet from the source to the relay corresponding to the jth MBM-TU. Let $\mathbf{H}_{sr}^j = [\mathbf{h}_1^{j,sr} \ \mathbf{h}_2^{j,sr} \ \cdots \ \mathbf{h}_{N_m}^{j,sr}]$ denote the $n_r \times N_m$ channel matrix from the jth MBM-TU of the source to the relay. Let $\mathbf{H}_{sr} = [\mathbf{H}_{sr}^1 \ \mathbf{H}_{sr}^2 \ \cdots \ \mathbf{H}_{sr}^{n_{tu}}]$ denote the overall $n_r \times N_m n_{tu}$ channel matrix between the source and the relay.

R to D channel: Let $\mathbf{h}_k^{j,rd} = [h_{1,k}^{j,rd} \ h_{2,k}^{j,rd} \ \cdots \ h_{n_d,k}^{j,rd}]^T$ denote the $n_d \times 1$-sized channel gain vector at the receiver of the destination node corresponding to the kth MAP of the jth MBM-TU of the relay node. The $h_{i,k}^{j,rd}$s are assumed to be i.i.d. and distributed as $\mathcal{CN}(0,1)$. Similar to those in the S to R channel, let $\mathbb{H}_{rd}^j$, $\mathbf{H}_{rd}^j$, and $\mathbf{H}_{rd}$ denote the MBM channel alphabet, $n_d \times N_m$ channel matrix, and $n_d \times N_m n_{tu}$ overall channel matrix, respectively.

R to R-SI channel: Let $\mathbf{h}_k^{j,rr} = [h_{1,k}^{j,rr} \ h_{2,k}^{j,rr} \ \cdots \ h_{n_r,k}^{j,rr}]^T$ denote the $n_r \times 1$-sized SI channel gain vector corresponding to the kth MAP of the jth MBM-TU at the relay. The $h_{i,k}^{j,rr}$s are modeled as i.i.d. and distributed as $\mathcal{CN}\left(0, (E/\sigma^2)^{-\lambda}\right)$ by assuming that the SI cancellation scheme completely removes the line-of-sight-component [9], where σ^2 denotes the average noise power and λ is a small positive constant that captures the quality of the SI cancellation technique [2],[9]. For example, $\lambda = 0$ and $\lambda = 1$ refers to poor and high quality SI cancellation techniques, respectively. Similar to those in the S to R channel, let $\mathbb{H}_{rr}^j$, $\mathbf{H}_{rr}^j$, and $\mathbf{H}_{rr}$ denote the MBM SI channel alphabet, $n_r \times N_m$ SI channel matrix, and $n_r \times N_m n_{tu}$ overall SI channel matrix, respectively.

D. Received signal

Let $s_j^{s,1}$ and $l_j^{s,1}$ denote the transmitted symbol and index of the selected MAP, respectively, on the jth MBM-TU of source node in the first phase. The $n_r \times 1$ received signal vector $\mathbf{y}_r^1$ at relay in the first phase can be written as

$$
\begin{aligned}
\mathbf{y}_r^1 &= \underbrace{\sum_{j=1}^{n_{tu}} s_j^{s,1} \mathbf{h}_{l_j^{s,1}}^{j,sr}}_{\text{desired signal}} + \underbrace{\sum_{j=1}^{n_{tu}} s_j^{r,1} \mathbf{h}_{l_j^{r,1}}^{j,rr}}_{\text{SI signal}} + \mathbf{n}_r^1 \\
&= \sum_{j=1}^{n_{tu}} s_j^{s,1} \mathbf{H}_{sr}^j \mathbf{e}_{l_j^{s,1}} + \sum_{j=1}^{n_{tu}} s_j^{r,1} \mathbf{H}_{rr}^j \mathbf{e}_{l_j^{r,1}} + \mathbf{n}_r^1 \\
&= \mathbf{H}_{sr} \mathbf{x}^{s,1} + \mathbf{H}_{rr} \mathbf{x}^{r,1} + \mathbf{n}_r^1,
\end{aligned}
\tag{2}
$$

where $s_j^{r,1}$ and $l_j^{r,1}$ denote the transmitted symbol and index of the selected MAP, respectively, on the jth MBM-TU of the relay to the destination in the first phase (which causes SI), $\mathbf{e}_p$ is an $N_m \times 1$ vector whose pth coordinate is 1 and all other coordinates are zero, $\mathbf{n}_r^1$ is the additive noise vector whose elements are i.i.d. and distributed as $\mathcal{CN}(0, \sigma^2)$, $\mathbf{x}^{s,1}$ and $\mathbf{x}^{r,1}$ are the $N_m n_{tu} \times 1$ transmit vectors belong to the GSM-MBM signal set $\mathbb{S}_{\text{gsm-mbm}}$, which is given by

$$
\mathbb{S}_{\text{gsm-mbm}} = \big\{ \mathbf{x} = [\mathbf{x}_1^T \ \mathbf{x}_2^T \ \cdots \ \mathbf{x}_{n_{tu}}^T]^T : \mathbf{x}_j = s_j \mathbf{e}_{l_j},
$$
$$
l_j \in \{1, \cdots, N_m\}; \ \mathbf{s} = [s_1 \ s_2 \ \cdots \ s_{n_{tu}}]^T \in \mathbb{S}_{\text{gsm}} \big\}. \tag{3}
$$

The size of the GSM-MBM signal set is $|\mathbb{S}_{\text{gsm-mbm}}| = 2^\eta$, where η is given by (1). Note that $\mathbf{x}^{s,1}$ and $\mathbf{x}^{r,1}$ are independent of each other, since $\mathbf{x}^{r,1}$ is the estimate of the previous data transmitted by the source. The relay detects the source signal $\mathbf{x}^{s,1}$ using the interference-oblivious ML detector, whose decision rule is given by

$$
\mathbf{x}^{r,2} = \underset{\mathbf{x} \in \mathbb{S}_{\text{gsm-mbm}}}{\operatorname{argmax}} \ P(\mathbf{y}_r^1 | \mathbf{H}_{sr}, \mathbf{x}) = \underset{\mathbf{x} \in \mathbb{S}_{\text{gsm-mbm}}}{\operatorname{argmin}} \ \|\mathbf{y}_r^1 - \mathbf{H}_{sr} \mathbf{x}\|^2. \tag{4}
$$

In the next phase, the relay forwards the detected data $\mathbf{x}^{r,2}$ to the destination. Then, the $n_d \times 1$ received signal vector $\mathbf{y}_d^2$ at the destination node in the second phase is given by

$$
\mathbf{y}_d^2 = \mathbf{H}_{rd} \mathbf{x}^{r,2} + \mathbf{n}_d^2, \tag{5}
$$

where $\mathbf{n}_d^2$ denotes the additive noise vector whose elements are i.i.d. and distributed as $\mathcal{CN}(0, \sigma^2)$. At the destination, the ML decision rule is given by

$$
\mathbf{x}^{d,2} = \underset{\mathbf{x} \in \mathbb{S}_{\text{gsm-mbm}}}{\operatorname{argmin}} \ \|\mathbf{y}_d^2 - \mathbf{H}_{rd} \mathbf{x}\|^2. \tag{6}
$$

Note that $\mathbf{x}^{d,2}$ is the estimate of $\mathbf{x}^{s,1}$. The bits corresponding to $\mathbf{x}^{d,2}$ are demapped as follows: i) the MBM-TU activation pattern for $\mathbf{s}^{d,2}$ gives $\lfloor \log_2 \binom{n_{tu}}{n_{rf}} \rfloor$ MBM-TU index bits, ii) the non-zero entries in $\mathbf{s}^{d,2}$ gives $n_{rf} \log_2 M$ QAM/PSK bits, and iii) for each non-zero location j in $\mathbf{s}^{d,2}$, $l_j^{d,2}$ gives m_{rf} mirror index bits; since $\mathbf{s}^{d,2}$ has n_{rf} non-zero entries, a total of $n_{rf} m_{rf}$ mirror index bits are obtained from $l_j^{d,2}$s.

III. PERFORMANCE ANALYSIS

In this section, we analyze the end-to-end average BEP performance and the diversity order achieved by the FDR-MBM system described in Sec. II. All the transmit vectors are assumed to be equally likely.

A. Average BEP analysis

Let $\mathbf{b}$ denote the $\eta \times 1$ bit vector transmitted by the source node. Let $\hat{\mathbf{b}}$ denote the estimate of $\mathbf{b}$ at the destination. Then, the end-to-end average BEP can be written as

$$
\begin{aligned}
P_B &= P(\hat{\mathbf{b}} \neq \mathbf{b}) \\
&= \sum_{\mathbf{x}} \sum_{\hat{\mathbf{x}}} P(\hat{\mathbf{b}} \neq \mathbf{b}, \mathbf{x}^{s,1} = \mathbf{x}, \mathbf{x}^{d,2} = \hat{\mathbf{x}}) \\
&= \frac{1}{2^\eta} \sum_{\mathbf{x}} \sum_{\hat{\mathbf{x}}} P(\hat{\mathbf{b}} \neq \mathbf{b}|\mathbf{x}^{s,1} = \mathbf{x}, \mathbf{x}^{d,2} = \hat{\mathbf{x}}) \times \\
&\qquad\qquad\qquad P(\mathbf{x}^{d,2} = \hat{\mathbf{x}}|\mathbf{x}^{s,1} = \mathbf{x}) \\
&= \frac{1}{2^\eta} \sum_{\mathbf{x}} \sum_{\hat{\mathbf{x}}} P(\mathbf{x}^{d,2} = \hat{\mathbf{x}}|\mathbf{x}^{s,1} = \mathbf{x}) \frac{\delta(\mathbf{x}, \hat{\mathbf{x}})}{\eta} \\
&= \frac{1}{2^\eta} \sum_{\mathbf{x}} \sum_{\hat{\mathbf{x}}} \sum_{\tilde{\mathbf{x}}} P(\mathbf{x}^{r,2} = \tilde{\mathbf{x}}|\mathbf{x}^{s,1} = \mathbf{x}) \times \\
&\qquad P(\mathbf{x}^{d,2} = \hat{\mathbf{x}}|\mathbf{x}^{r,2} = \tilde{\mathbf{x}}, \mathbf{x}^{s,1} = \mathbf{x}) \frac{\delta(\mathbf{x}, \hat{\mathbf{x}})}{\eta} \\
&= \frac{1}{2^\eta} \sum_{\mathbf{x}} \sum_{\hat{\mathbf{x}} \neq \mathbf{x}} \sum_{\tilde{\mathbf{x}}} \underbrace{P(\mathbf{x}^{r,2} = \tilde{\mathbf{x}}|\mathbf{x}^{s,1} = \mathbf{x})}_{\triangleq P_{sr}(\tilde{\mathbf{x}}|\mathbf{x})} \times \\
&\qquad \underbrace{P(\mathbf{x}^{d,2} = \hat{\mathbf{x}}|\mathbf{x}^{r,2} = \tilde{\mathbf{x}})}_{\triangleq P_{rd}(\hat{\mathbf{x}}|\tilde{\mathbf{x}})} \frac{\delta(\mathbf{x}, \hat{\mathbf{x}})}{\eta}, \quad (7)
\end{aligned}
$$

where $\delta(\mathbf{x}, \hat{\mathbf{x}})$ is the number of bits in which $\mathbf{x}$ differs from $\hat{\mathbf{x}}$, $1 \leq \delta(\mathbf{x}, \hat{\mathbf{x}}) \leq \eta$ when $\mathbf{x} \neq \hat{\mathbf{x}}$, $\delta(\mathbf{x}, \mathbf{x}) = 0$, the equality in (7) follows from the fact that $\mathbf{x}^{d,2}$ and $\mathbf{x}^{s,1}$ are independent given $\mathbf{x}^{r,2}$, $P_{sr}(\tilde{\mathbf{x}}|\mathbf{x})$ is the probability of the source's transmitted vector $\mathbf{x}^{s,1} = \mathbf{x}$ being decoded as $\mathbf{x}^{r,2} = \tilde{\mathbf{x}}$ at the relay, and $P_{rd}(\hat{\mathbf{x}}|\tilde{\mathbf{x}})$ is the probability of the relay's transmitted vector $\mathbf{x}^{r,2} = \tilde{\mathbf{x}}$ being decoded as $\mathbf{x}^{d,2} = \hat{\mathbf{x}}$ at the destination.

Derivation of $P_{sr}(\tilde{\mathbf{x}}|\mathbf{x})$: $P_{sr}(\tilde{\mathbf{x}}|\mathbf{x})$ can be written as

$$
\begin{aligned}
P_{sr}(\tilde{\mathbf{x}}|\mathbf{x}) &= \sum_{\bar{\mathbf{x}}} P_{sr}(\mathbf{x}^{r,2} = \tilde{\mathbf{x}}|\mathbf{x}^{s,1} = \mathbf{x}, \mathbf{x}^{r,1} = \bar{\mathbf{x}}) \times \\
&\qquad\qquad P(\mathbf{x}^{r,1} = \bar{\mathbf{x}}|\mathbf{x}^{s,1} = \mathbf{x}) \\
&= \frac{1}{2^\eta} \sum_{\bar{\mathbf{x}}} \underbrace{P_{sr}(\mathbf{x}^{r,2} = \tilde{\mathbf{x}}|\mathbf{x}^{s,1} = \mathbf{x}, \mathbf{x}^{r,1} = \bar{\mathbf{x}})}_{\triangleq P_{sr}(\tilde{\mathbf{x}}|\mathbf{x},\bar{\mathbf{x}})}, \quad (8)
\end{aligned}
$$

where the equality in (8) follows from the fact that $\mathbf{x}^{r,1}$ and $\mathbf{x}^{s,1}$ are independent, and $P_{sr}(\tilde{\mathbf{x}}|\mathbf{x}, \bar{\mathbf{x}})$ is the probability of the source's transmitted vector $\mathbf{x}^{s,1} = \mathbf{x}$ being decoded as $\mathbf{x}^{r,2} = \tilde{\mathbf{x}}$ at the relay given that relay transmitted $\mathbf{x}^{r,1} = \bar{\mathbf{x}}$. The probability $P_{sr}(\tilde{\mathbf{x}}|\mathbf{x}, \bar{\mathbf{x}})$ can be written as

$$
P_{sr}(\tilde{\mathbf{x}}|\mathbf{x}, \bar{\mathbf{x}}) = \mathbb{E}_{\mathbf{H}_{sr}}\left\{ P_{sr}(\tilde{\mathbf{x}}|\mathbf{x}, \bar{\mathbf{x}}, \mathbf{H}_{sr}) \right\}, \quad (9)
$$

where $\mathbb{E}\{.\}$ denotes the expectation operator. From (2) and (4), the probability $P_{sr}(\tilde{\mathbf{x}}|\mathbf{x}, \bar{\mathbf{x}}, \mathbf{H}_{sr})$ can be written as

$$
P_{sr}(\tilde{\mathbf{x}}|\mathbf{x}, \bar{\mathbf{x}}, \mathbf{H}_{sr}) = P\left(\bigcap_{\mathbf{x}' \neq \tilde{\mathbf{x}}} \left\{ \begin{matrix} \|\mathbf{H}_{sr}(\mathbf{x}-\tilde{\mathbf{x}})+\tilde{\mathbf{n}}_r^1\|^2 < \\ \|\mathbf{H}_{sr}(\mathbf{x}-\mathbf{x}')+\tilde{\mathbf{n}}_r^1\|^2 \end{matrix} \right\} \right), (10)
$$

where $\tilde{\mathbf{n}}_r^1 = \mathbf{H}_{rr}\bar{\mathbf{x}} + \mathbf{n}_r^1$. It is easy to see that $\tilde{\mathbf{n}}_r^1 \sim \mathcal{CN}\left(\mathbf{0}_{n_r \times 1}, (\sigma^2 + \|\bar{\mathbf{x}}\|^2(E/\sigma^2)^{-\lambda})\mathbf{I}_{n_r}\right)$, where $\mathbf{0}_{p \times 1}$ denotes the all zero vector of size $p \times 1$ and $\mathbf{I}_p$ denotes the $p \times p$ identity matrix. Using the monotonicity property (i.e., $P(\cap_k A_k) \leq P(A_k)$), the probability in (10) can be upper bounded as

$$
P_{sr}(\tilde{\mathbf{x}}|\mathbf{x}, \bar{\mathbf{x}}, \mathbf{H}_{sr}) \leq \begin{cases} P\left(\begin{matrix} \|\mathbf{H}_{sr}(\mathbf{x}-\tilde{\mathbf{x}})+\tilde{\mathbf{n}}_r^1\|^2 \\ < \|\tilde{\mathbf{n}}_r^1\|^2 \end{matrix}\right) & \text{if } \mathbf{x} \neq \tilde{\mathbf{x}} \\ \min_{\mathbf{x}' \neq \mathbf{x}} P\left(\begin{matrix} \|\mathbf{H}_{sr}(\mathbf{x}-\mathbf{x}')+\tilde{\mathbf{n}}_r^1\|^2 \\ > \|\tilde{\mathbf{n}}_r^1\|^2 \end{matrix}\right) & \text{if } \mathbf{x} = \tilde{\mathbf{x}} \end{cases}
$$

$$
= \begin{cases} Q\left(\sqrt{\frac{\|\mathbf{H}_{sr}(\mathbf{x}-\tilde{\mathbf{x}})\|^2}{2(\sigma^2+\|\bar{\mathbf{x}}\|^2(E/\sigma^2)^{-\lambda})}}\right) & \text{if } \mathbf{x} \neq \tilde{\mathbf{x}} \\ 1 - \max_{\mathbf{x}' \neq \mathbf{x}} Q\left(\sqrt{\frac{\|\mathbf{H}_{sr}(\mathbf{x}-\mathbf{x}')\|^2}{2(\sigma^2+\|\bar{\mathbf{x}}\|^2(E/\sigma^2)^{-\lambda})}}\right) & \text{if } \mathbf{x} = \tilde{\mathbf{x}} \end{cases}, \quad (11)
$$

where $Q(x) = \frac{1}{\sqrt{2\pi}} \int_x^\infty e^{-\frac{t^2}{2}} dt$. Substituting (11) in (9) and simplifying [15], we get

$$
P_{sr}(\tilde{\mathbf{x}}|\mathbf{x}, \bar{\mathbf{x}}) \leq \begin{cases} g_{n_r}\left(\frac{\|\mathbf{x}-\tilde{\mathbf{x}}\|^2}{4(\sigma^2+\|\bar{\mathbf{x}}\|^2(E/\sigma^2)^{-\lambda})}\right) & \text{if } \mathbf{x} \neq \tilde{\mathbf{x}} \\ 1 - \max_{\mathbf{x}' \neq \mathbf{x}} g_{n_r}\left(\frac{\|\mathbf{x}-\mathbf{x}'\|^2}{4(\sigma^2+\|\bar{\mathbf{x}}\|^2(E/\sigma^2)^{-\lambda})}\right) & \text{if } \mathbf{x} = \tilde{\mathbf{x}} \end{cases}
$$

$$
= \begin{cases} g_{n_r}\left(\frac{\|\mathbf{x}-\tilde{\mathbf{x}}\|^2}{4(\sigma^2+\|\bar{\mathbf{x}}\|^2(E/\sigma^2)^{-\lambda})}\right) & \text{if } \mathbf{x} \neq \tilde{\mathbf{x}} \\ 1 - g_{n_r}\left(\frac{\min_{\mathbf{x}' \neq \mathbf{x}} \|\mathbf{x}-\mathbf{x}'\|^2}{4(\sigma^2+\|\bar{\mathbf{x}}\|^2(E/\sigma^2)^{-\lambda})}\right) & \text{if } \mathbf{x} = \tilde{\mathbf{x}} \end{cases}, \quad (12)
$$

where

$$
g_k(\beta) = f(\beta)^k \sum_{i=0}^{k-1} \binom{k-1+i}{i} (1 - f(\beta))^i, \quad (13)
$$

$f(\beta) = \frac{1}{2}\left(1 - \sqrt{\frac{\beta}{1+\beta}}\right)$, and the equality in (12) follows from the monotonically non-increasing nature of $g_k(\beta)$.

Derivation of $P_{rd}(\hat{\mathbf{x}}|\tilde{\mathbf{x}})$: Following similar steps from (9)-(12), the $P_{rd}(\hat{\mathbf{x}}|\tilde{\mathbf{x}})$ can be upper bounded as

$$
P_{rd}(\hat{\mathbf{x}}|\tilde{\mathbf{x}}) \leq \begin{cases} \mathbb{E}_{\mathbf{H}_{rd}}\left\{ Q\left(\sqrt{\frac{\|\mathbf{H}_{rd}(\hat{\mathbf{x}}-\tilde{\mathbf{x}})\|^2}{2\sigma^2}}\right) \right\} & \text{if } \hat{\mathbf{x}} \neq \tilde{\mathbf{x}} \\ 1 - \max_{\mathbf{x}' \neq \tilde{\mathbf{x}}} \mathbb{E}_{\mathbf{H}_{rd}}\left\{ Q\left(\sqrt{\frac{\|\mathbf{H}_{rd}(\tilde{\mathbf{x}}-\mathbf{x}')\|^2}{2\sigma^2}}\right) \right\} & \text{if } \hat{\mathbf{x}} = \tilde{\mathbf{x}} \end{cases} \quad (14)
$$

$$
= \begin{cases} g_{n_d}\left(\frac{\|\hat{\mathbf{x}}-\tilde{\mathbf{x}}\|^2}{4\sigma^2}\right) & \text{if } \hat{\mathbf{x}} \neq \tilde{\mathbf{x}} \\ 1 - g_{n_d}\left(\frac{\min_{\mathbf{x}' \neq \tilde{\mathbf{x}}} \|\tilde{\mathbf{x}}-\mathbf{x}'\|^2}{4\sigma^2}\right) & \text{if } \hat{\mathbf{x}} = \tilde{\mathbf{x}} \end{cases}. \quad (15)
$$

Substituting (8), (12), and (15) in (7) gives an upper bound on the end-to-end average BEP. Next, we derive the diversity order achieved by the FDR-MBM system.

B. Diversity analysis

In this subsection, we derive lower and upper bounds on diversity order denoted by d and show that these bounds turn out to be the same, given by $\min\{n_r(\min\{\lambda, 1\}), n_d\}$.

1) Lower bound on d: Using Craig's formula [15], the expectation of $Q(.)$ function in (11) can be written as

$$
\begin{aligned}
&\mathbb{E}_{\mathbf{H}_{sr}}\left\{ Q\left(\sqrt{\frac{\|\mathbf{H}_{sr}(\mathbf{x}-\tilde{\mathbf{x}})\|^2}{2(\sigma^2+\|\bar{\mathbf{x}}\|^2(E/\sigma^2)^{-\lambda})}}\right) \right\} \\
&= \mathbb{E}_{\mathbf{H}_{sr}}\left\{ \frac{1}{\pi} \int_{\theta=0}^{\pi/2} \exp\left(\frac{-\|\mathbf{H}_{sr}(\mathbf{x}-\tilde{\mathbf{x}})\|^2}{4(\sigma^2+\|\bar{\mathbf{x}}\|^2(E/\sigma^2)^{-\lambda})\sin^2(\theta)}\right) d\theta \right\} \\
&= \frac{1}{\pi} \int_{\theta=0}^{\pi/2} \mathbb{E}_{\mathbf{H}_{sr}}\left\{ \exp\left(\frac{-\|\mathbf{H}_{sr}(\mathbf{x}-\tilde{\mathbf{x}})\|^2}{4(\sigma^2+\|\bar{\mathbf{x}}\|^2(E/\sigma^2)^{-\lambda})\sin^2(\theta)}\right) \right\} d\theta
\end{aligned}
$$

$$= \frac{1}{\pi}\int_{\theta=0}^{\pi/2}\left(1+\frac{\|\mathbf{x}-\tilde{\mathbf{x}}\|^2}{4\big(\sigma^2+\|\bar{\mathbf{x}}\|^2(E/\sigma^2)^{-\lambda}\big)\sin^2(\theta)}\right)^{-n_r}d\theta. \quad (16)$$

Since $\frac{\|\mathbf{x}-\tilde{\mathbf{x}}\|^2}{4(\sigma^2+\|\bar{\mathbf{x}}\|^2(E/\sigma^2)^{-\lambda})\sin^2(\theta)}\gg 1$ at high SNRs (i.e., 1 can be neglected in (16)), we can write

$$\mathbb{E}_{\mathbf{H}_{sr}}\left\{Q\left(\sqrt{\frac{\|\mathbf{H}_{sr}(\mathbf{x}-\tilde{\mathbf{x}})\|^2}{2\big(\sigma^2+\|\bar{\mathbf{x}}\|^2(E/\sigma^2)^{-\lambda}\big)}}\right)\right\}$$

$$\approx\left(\frac{1}{\sigma^2}\right)^{-n_r\min\{\lambda,1\}}c_{\mathbf{x},\tilde{\mathbf{x}},\hat{\mathbf{x}},E,\lambda,n_r}, \quad (17)$$

where $c_{\mathbf{x},\tilde{\mathbf{x}},\hat{\mathbf{x}},E,\lambda,n_r}$ is some constant and it is independent of σ^2, and $\min\{1,\lambda\}$ is due to the fact $\sigma^2\ll 1$ (therefore, $\sigma^2+\|\bar{\mathbf{x}}\|^2(E/\sigma^2)^{-\lambda}$ in (16) is dominated by the smallest power). Similarly, we can write

$$\mathbb{E}_{\mathbf{H}_{rd}}\left\{Q\left(\sqrt{\frac{\|\mathbf{H}_{rd}(\hat{\mathbf{x}}-\tilde{\mathbf{x}})\|^2}{2\sigma^2}}\right)\right\}\approx\left(\frac{1}{\sigma^2}\right)^{-n_d}c_{\hat{\mathbf{x}},\tilde{\mathbf{x}},n_d}. \quad (18)$$

Substituting (8), (9), (11), (14), (17), (18), $P_{sr}(\mathbf{x}|\mathbf{x},\bar{\mathbf{x}})\leq 1$, and $P_{rd}(\tilde{\mathbf{x}}|\tilde{\mathbf{x}})\leq 1$ in (7), and simplifying, we get

$$P_B\leq\frac{1}{2^{2\eta}}\sum_{\mathbf{x}}\sum_{\hat{\mathbf{x}}\neq\mathbf{x}}\sum_{\bar{\mathbf{x}}}\left\{\left(\frac{1}{\sigma^2}\right)^{-n_d}c_{\hat{\mathbf{x}},\mathbf{x},n_d}+\left(\frac{1}{\sigma^2}\right)^{-n_r\min\{\lambda,1\}}c_{\mathbf{x},\hat{\mathbf{x}},\bar{\mathbf{x}},E,\lambda,n_r}\right.$$

$$\left.+\sum_{\tilde{\mathbf{x}}\neq\mathbf{x},\hat{\mathbf{x}}}\left(\frac{1}{\sigma^2}\right)^{-(n_r\min\{\lambda,1\}+n_d)}c_{\mathbf{x},\tilde{\mathbf{x}},\bar{\mathbf{x}},E,\lambda,n_r}c_{\hat{\mathbf{x}},\tilde{\mathbf{x}},n_d}\right\}\frac{\delta(\mathbf{x},\hat{\mathbf{x}})}{\eta}, \quad (19)$$

which shows that the diversity order of P_B is lower bounded by $\min\{n_d,n_r(\min\{\lambda,1\}),n_r\min\{\lambda,1\}+n_d\}=\min\{n_r\min\{\lambda,1\},n_d\}$, i.e.,

$$d\geq\min\{n_r(\min\{\lambda,1\}),n_d\}. \quad (20)$$

2) Upper bound on d: The average BEP in (7) can be lower bounded as

$$P_B\geq\frac{1}{\eta2^{2\eta}}\sum_{\mathbf{x}}\sum_{\bar{\mathbf{x}}}\sum_{\tilde{\mathbf{x}}\neq\mathbf{x}}P_{sr}(\tilde{\mathbf{x}}|\mathbf{x},\bar{\mathbf{x}})\left\{\sum_{\hat{\mathbf{x}}\neq\mathbf{x}}P_{rd}(\hat{\mathbf{x}}|\tilde{\mathbf{x}})\right\}+R_1 \quad (21)$$

$$\geq\frac{1}{\eta2^{2\eta}}\sum_{\mathbf{x}}\sum_{\bar{\mathbf{x}}}\sum_{\tilde{\mathbf{x}}\neq\mathbf{x}}P_{sr}(\tilde{\mathbf{x}}|\mathbf{x},\bar{\mathbf{x}})\big(1-P_{rd}(\mathbf{x}|\tilde{\mathbf{x}})\big) \quad (22)$$

$$\geq\frac{1}{\eta2^{2\eta+1}}\sum_{\mathbf{x}}\sum_{\bar{\mathbf{x}}}\left\{\sum_{\tilde{\mathbf{x}}\neq\mathbf{x}}P_{sr}(\tilde{\mathbf{x}}|\mathbf{x},\bar{\mathbf{x}})\right\} \quad (23)$$

$$=\frac{1}{\eta2^{2\eta+1}}\sum_{\mathbf{x}}\sum_{\bar{\mathbf{x}}}\left\{P_{sr}(\mathbf{x}^{r,2}\neq\mathbf{x}|\mathbf{x},\bar{\mathbf{x}})\right\}$$

$$\geq\frac{1}{\eta2^{2\eta+1}}\sum_{\mathbf{x}}\sum_{\bar{\mathbf{x}}}\mathbb{E}_{\mathbf{H}_{sr}}\left\{P\big(\|\mathbf{H}_{sr}(\mathbf{x}-\mathbf{x}'')+\tilde{\mathbf{n}}_r^1\|^2<\|\tilde{\mathbf{n}}_r^1\|^2\big)\right\} \quad (24)$$

$$=\frac{1}{\eta2^{2\eta+1}}\sum_{\mathbf{x}}\sum_{\bar{\mathbf{x}}}\mathbb{E}_{\mathbf{H}_{sr}}\left\{Q\left(\sqrt{\frac{\|\mathbf{H}_{sr}(\mathbf{x}-\mathbf{x}'')\|^2}{2\big(\sigma^2+\|\bar{\mathbf{x}}\|^2(E/\sigma^2)^{-\lambda}\big)}}\right)\right\}, \quad (25)$$

where R_1 denotes the remaining summation, the inequality in (21) follows from $\delta(\mathbf{x},\hat{\mathbf{x}})\geq 1$, the inequality in (22) follows from $R_1\geq 0$, the inequality in (23) follows from the fact $P_{rd}(\mathbf{x}|\tilde{\mathbf{x}})\leq 0.5$ when $\mathbf{x}\neq\tilde{\mathbf{x}}$ (because $Q(.)\leq 0.5$), $\mathbf{x}''$ is any transmit vector other than $\mathbf{x}$, and the inequality in (24) follows from the monotonicity property of the probability. Substituting (17) in (25), at high SNRs, we have

$$P_B\geq\frac{1}{\eta2^{2\eta+1}}\sum_{\mathbf{x}}\sum_{\bar{\mathbf{x}}}\left(\frac{1}{\sigma^2}\right)^{-n_r\min\{\lambda,1\}}c_{\mathbf{x},\mathbf{x}'',\bar{\mathbf{x}},E,\lambda,n_r},$$
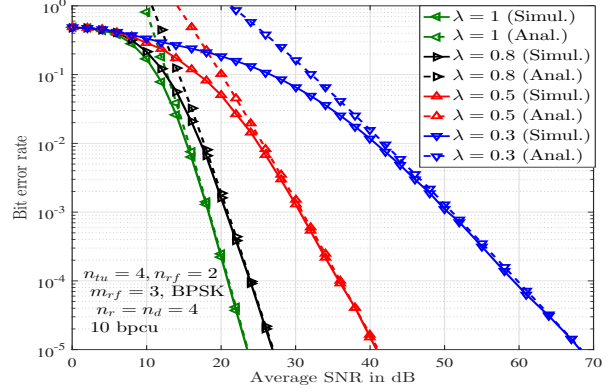

Fig. 3. BER performance comparison between analytical BER upper bound and simulated BER of the FDR-MBM system with $n_{tu}=4, n_{rf}=2, m_{rf}=3$, BPSK, $n_r=n_d=4$, $\lambda=1,0.8,0.5,0.3$, and 10 bpcu.

which shows that the diversity order of P_B is upper bounded by $n_r(\min\{\lambda,1\})$, i.e.,

$$d\leq n_r(\min\{\lambda,1\}). \quad (26)$$

Similarly, the other upper bound n_d (i.e., $d\leq n_d$) can be obtained as follows:

$$P_B\geq\frac{1}{\eta2^{2\eta}}\sum_{\tilde{\mathbf{x}}}\sum_{\bar{\mathbf{x}}}\sum_{\hat{\mathbf{x}}\neq\tilde{\mathbf{x}}}P_{rd}(\hat{\mathbf{x}}|\tilde{\mathbf{x}})\left\{\sum_{\mathbf{x}\neq\hat{\mathbf{x}}}P_{sr}(\tilde{\mathbf{x}}|\mathbf{x},\bar{\mathbf{x}})\right\}+R_2 \quad (27)$$

$$\geq\frac{1}{\eta2^{2\eta}}\sum_{\tilde{\mathbf{x}}}\sum_{\bar{\mathbf{x}}}\sum_{\hat{\mathbf{x}}\neq\tilde{\mathbf{x}}}P_{rd}(\hat{\mathbf{x}}|\tilde{\mathbf{x}})\left\{1-P_{sr}(\tilde{\mathbf{x}}|\hat{\mathbf{x}},\bar{\mathbf{x}})\right\} \quad (28)$$

$$\geq\frac{1}{\eta2^{\eta+1}}\sum_{\tilde{\mathbf{x}}}\sum_{\hat{\mathbf{x}}\neq\tilde{\mathbf{x}}}P_{rd}(\hat{\mathbf{x}}|\tilde{\mathbf{x}}) \quad (29)$$

$$\geq\frac{1}{\eta2^{\eta+1}}\sum_{\tilde{\mathbf{x}}}\mathbb{E}_{\mathbf{H}_{rd}}\left\{Q\left(\sqrt{\frac{\|\mathbf{H}_{rd}(\mathbf{x}'''-\tilde{\mathbf{x}})\|^2}{2\sigma^2}}\right)\right\} \quad (30)$$

$$\approx\frac{1}{\eta2^{\eta+1}}\sum_{\tilde{\mathbf{x}}}\left(\frac{1}{\sigma^2}\right)^{-n_d}c_{\mathbf{x}''',\tilde{\mathbf{x}},n_d}, \quad (31)$$

where $\mathbf{x}'''$ is any transmit vector other than $\tilde{\mathbf{x}}$. (31) shows that the diversity order of P_B is upper bounded by n_d, i.e.,

$$d\leq n_d. \quad (32)$$

From (26) and (32), the diversity order d is upper bounded by

$$d\leq\min\{n_r(\min\{\lambda,1\}),n_d\}. \quad (33)$$

Finally, from (20) and (33), we see that the diversity order (d) achieved by the FDR-MBM system is $\min\{n_r(\min\{\lambda,1\}),n_d\}$.

IV. RESULTS AND DISCUSSIONS

In this section, we present the numerical results that validate the tightness of the analytical upper bound on the average BEP and the diversity order achieved by the FDR-MBM system.

In Fig. 3, we illustrate the tightness of the upper bound on the end-to-end average BEP of the FDR-MBM system with $n_{tu}=4$, $n_{rf}=2$, $m_{rf}=3$, BPSK, $n_r=n_d=4$, and 10 bpcu for various values of $\lambda=1,0.8,0.5,0.3$. It can be seen that the analytical upper bound becomes tight as SNR increases. It is also seen that, as expected, the performance degrades as λ decreases (i.e., quality of SI cancellation technique). For example, to achieve 10^{-5} BER, the average
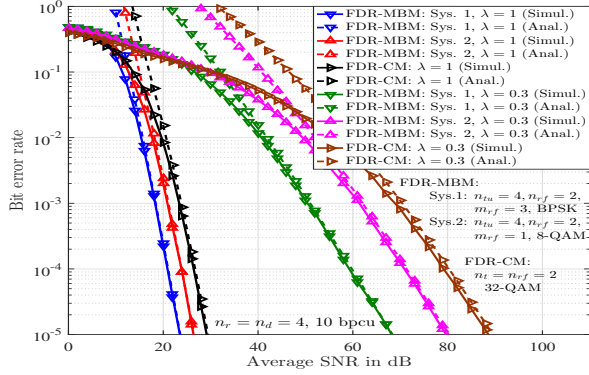
Fig. 4. BER performance comparison between FDR-MBM and FDR-CM with $n_r = n_d = 4$ and 10 bpcu. FDR-MBM: $n_{tu} = 4$, $n_{rf} = 2$, $i)$ $m_{rf} = 3$, BPSK, $ii)$ $m_{rf} = 1$, 8-QAM; FDR-CM: $n_t = n_{rf} = 2$, 32-QAM.
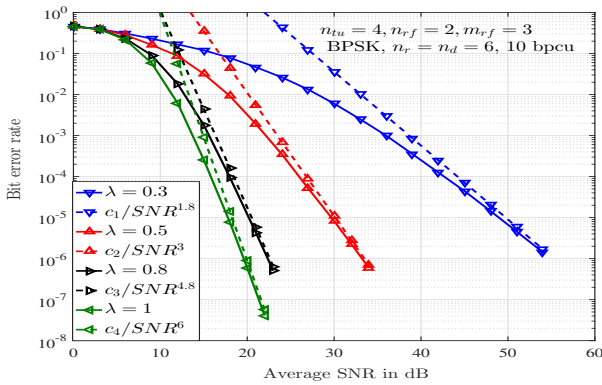

Fig. 5. Diversity orders achieved by FDR-MBM with $n_{tu} = 4$, $n_{rf} = 2$, $m_{rf} = 3$, BPSK, $n_r = n_d = 6$, and 10 bpcu for various values of λ: $\lambda = 1, 0.8, 0.5, 0.3$.

SNR required is about 23 dB, 27 dB, 41 dB, and 68 dB for $\lambda = 1, 0.8, 0.5$, and 0.3, respectively.

Figure 4 shows the BER performance comparison between FDR-MBM and FDR-CM systems. Both the systems use $\lambda = 1, 0.3$, $n_r = n_d = 4$, 10 bpcu, and ML detection. The considered system parameters are as follows. FDR-MBM: $n_{tu} = 4$, $n_{rf} = 2$, $i)$ $m_{rf} = 3$, BPSK, $ii)$ $m_{rf} = 1$, 8-QAM; FDR-CM: $n_t = n_{rf} = 2$, 32-QAM, where n_t denotes the number of transmit antennas. Note that FDR-MBM specializes to FDR-CM when $m_{rf} = 0$. It is seen that the analytical upper bound is tight at moderate to high SNRs for both the systems. Also, it is observed that FDR-MBM systems achieve better performance compared to FDR-CM. For example, to achieve 10^{-5} BER with $\lambda = 1$, FDR-MBM system-2 ($m_{rf} = 1$ and 8-QAM) requires about 2 dB less SNR compared to FDR-CM. This is because, to achieve the same spectral efficiency, FDR-MBM can use a smaller sized alphabet (8-QAM and BPSK) compared to FDR-CM (32-QAM). For the same reason, FDR-MBM system-1 (BPSK) performs better than FDR-MBM system-2 (8-QAM) by about 3 dB. Further, it is seen that the FDR-MBM is more robust to SI than FDR-CM. For example, at 10^{-5} BER, the performance of FDR-CM degrades by about 60 dB when λ is reduced to 0.3 from 1, whereas the degradation in FDR-MBM system-1 and FDR-MBM system-2 is only about 44 dB and 53 dB,

respectively.

In Fig. 5, we validate the diversity orders of FDR-MBM for various values of $\lambda = 1, 0.8, 0.5, 0.3$. The system parameters are $n_{tu} = 4, n_{rf} = 2, m_{rf} = 3$, BPSK, $n_r = n_d = 6$, and 10 bpcu. The constants used in the Fig. 5 are $c_1 = 9000$, $c_2 = 11000$, $c_3 = 70000$, and $c_4 = 9 * 10^5$. It can be seen that the slopes of the simulated BER plots in the high SNR regime (which are nothing but the diversity orders) match with the analytical diversity plots (i.e., $SNR^{-\min\{n_r \min\{\lambda,1\},n_d\}}$).

V. CONCLUSIONS

We analyzed the performance of a two-hop three-node FD relay network, where the source and relay nodes transmit using MBM. We referred to this system as FDR-MBM system. First, we derived an upper bound on the end-to-end average BEP of FDR-MBM with ML detection at the relay and destination nodes. This bound was shown to be increasingly tight with increasing SNR. Our numerical results showed that, for the same spectral efficiency, FDR-MBM achieves better performance compared to FD relaying with conventional modulation schemes. Next, we derived the diversity order achieved by the FDR-MBM system. The analytically predicted diversity order was also validated through simulations. Power allocation and relay selection in FDR-MBM systems can be taken up for future work.

REFERENCES

[1] J. I. Choi *et al.*, "Achieving single channel full-duplex wireless communication," in *Proc. ACM MobiCom'2010*, Sept. 2010, pp. 1-12.
[2] M. Duarte, C. Dick, and A. Sabharwal, "Experiment-driven characterization of full-duplex wireless systems," *IEEE Trans. Wireless Commun.*, vol. 11, no. 12, pp. 4296-4307, Dec. 2012.
[3] Z. Zhang *et al.*, "Full-duplex techniques for 5G networks: self-interference cancellation, protocol design, and relay selection," *IEEE Commun. Mag.*, vol. 53, no. 5, pp. 128-137, May 2015.
[4] L. J. Rodriguez, N. H. Tran, and T. Le-Ngoc, "Optimal power allocation and capacity of full-duplex AF relaying under residual self-interference," *IEEE Wireless Commun. Lett.*, vol. 3, no. 2, pp. 233-236, Apr. 2014.
[5] B. P. Day, A. Margetts, D. W. Bliss, and P. Schniter, "Full-duplex bidirectional MIMO: achievable rates under limited dynamic range," *IEEE Trans. Signal Process.*, vol. 60, no. 7, pp. 3702-3713, Jul. 2012.
[6] A. Nosratinia *et al.*, "Cooperative communication in wireless networks," *IEEE Commun. Mag.*, vol. 42, no. 10, pp. 74-80, Oct. 2004.
[7] I. Krikidis, H. A. Suraweera, S. Yang, and K. Berberidis, "Full-duplex relaying over block fading channel: a diversity perspective," *IEEE Trans. Wireless Commun.*, vol. 11, no. 12, pp. 4524-4535, Dec. 2012.
[8] L. J. Rodriguez, N. H. Tran, and T. Le-Ngoc, "Performance of full-duplex AF relaying in the presence of residual self-interference," *IEEE J. Sel. Areas Commun.*, vol. 32, no. 9, pp. 1752-1764, Sep. 2014.
[9] I. Krikidis and H. A. Suraweera, "Full-duplex cooperative diversity with Alamouti space-time code," *IEEE Wireless Commun. Lett.*, vol. 2. no. 5, pp. 519-522, Oct. 2013.
[10] G.-P. Liu, R. Yu, H. Ji, V. Leung, and X. Li, "In-band full-duplex relaying: a survey, research issues and challenges," *IEEE Commun. Surveys & Tuts.*, vol. 17, no. 2, pp. 500-524, 2015.
[11] S. Narayanan, H. Ahmadi, and M. F. Flanagan, "On the performance of spatial modulation MIMO for full-duplex relay networks," *IEEE Trans. Wireless Commun.*, vol. 16, no. 6, pp. 3727-3746, Jun. 2017.
[12] A. K. Khandani, "Media-based modulation: a new approach to wireless transmission," in *Proc. IEEE ISIT'2013*, Jul. 2013, pp. 3050-3054.
[13] Y. Naresh and A. Chockalingam, "On media-based modulation using RF mirrors," *IEEE Trans. Veh. Tech.*, vol. 66, pp. 4967-4983, Jun. 2017.
[14] Y. Naresh and A. Chockalingam, "Full-duplex media-based modulation," in *Proc. IEEE GLOBECOM'2017*, Dec. 2017, pp. 1-6.
[15] M.-S. Alouini and A. Goldsmith, "A unified approach for calculating error rates of linearly modulated signals over generalized fading channels," *IEEE Trans. Commun.*, vol. 47, no. 9, pp. 1324-1334, Sep. 1999.